Table IX. Final Positional Parameters for E_2ppz and A_2ppz

	x/a	*y/b*	*z/c*
		E_2ppz	
Pt(1)	0.19539 (6)	0.18337 (3)	0.16875 (5)
Cl(1)	0.39058 (82)	0.06707 (33)	0.23026 (73)
Cl(2)	-0.00759 (63)	0.29419 (28)	0.10441 (49)
N(1)	0.07392 (146)	0.07315 (77)	0.07215 (116)
C(1)	0.14694 (209)	0.06012 (92)	-0.07861 (148)
C(3)	0.17032 (232)	-0.02794 (94)	-0.32732 (149)
C(2)	0.07680 (170)	-0.01241 (91)	-0.15752 (141)
C(4)	0.40337 (244)	0.29757 (136)	0.17481 (212)
C(5)	0.25412 (290)	0.29158 (132)	0.32237 (223)
		A_2ppz	
Pt	0.17461 (3)	0.25951 (4)	0.16680 (2)
Cl(1)	0.00976 (21)	0.33738 (34)	0.19677 (19)
Cl(2)	0.33064 (27)	0.16844 (52)	0.12590 (25)
P	0.29499 (20)	0.41733 (33)	0.27359 (17)
N(1)	0.06622 (59)	0.10769 (93)	0.06362 (48)
C(1)	0.03221 (87)	-0.03412 (127)	0.08916 (65)
C(2)	-0.03311 (88)	-0.14501 (125)	0.02492 (64)
C(3)	-0.06993 (117)	-0.30398 (154)	0.05550 (77)
C(11)	0.23067 (92)	0.52549 (139)	0.34771 (79)
C(12)	0.31171 (143)	0.63850 (211)	0.41800 (110)
C(21)	0.42097 (108)	0.31128 (180)	0.34779 (97)
C(22)	0.39174 (174)	0.16409 (233)	0.39523 (112)
C(31)	0.35810 (112)	0.57408 (182)	0.22110 (94)
C(32)	0.26893 (170)	0.67686 (243)	0.15582 (143)

measured every 300 reflections to check the crystal orientation. Data were corrected for absorption by using the ψ scans of five reflections, $\bar{1}2\bar{2}$, $\bar{1}3\bar{3}$, $2\bar{4}\bar{4}$, $2\bar{5}\bar{6}$, and 266 ($\chi > 85.0°$). The range of transmission factors was 0.506-0.997. During the refinement (all atoms treated anisotropically) the contribution of the H atoms in their idealized positions (C-H = 0.98 Å, B_{iso} = 5.0 Å^2) was taken into account but not refined. Final positional parameters are listed in Table IX.

Acknowledgment. W.K. carried out our work during the tenure of a research fellowship from the Swiss National Science Foundation. A.A., F.I., and C.S. acknowledge the support of the Italian National Research Council. We are greatly indebted to Prof. P. S. Pregosin for much valuable discussion and F. Bangerter for NMR measurements.

Registry No. A_1mepz, 118516-01-1; A_1*mepz, 118516-02-2; A_1mpz, 118515-76-7; A_1*mpz, 118515-75-6; A_1opz, 118516-03-3; A_1phz, 118516-06-6; A_1ppz, 118515-74-5; A_1pz, 118515-73-4; A_1tpz, 118515-77-8; A_1trpz, 118516-05-5; A_1*trpz, 118516-04-4; A_2mepz, 118515-82-5; A_2mpz, 118515-85-8; A_2opz, 118515-83-6; A_2phz, 118515-88-1; A_2ppz, 118515-84-7; A_2pz, 118515-81-4; A_2tpz, 118515-87-0; A_2trpz, 118515-86-9; BN, 118515-92-7; B_1ppz, 118515-98-3; B_1pz, 118515-96-1; B_1tpz, 118515-99-4; B_2ppz, 118515-89-2; B_2pz, 118515-97-2; B_2tpz, 118516-00-0; C_1ppz, 118515-79-0; C_1pz, 118515-78-9; C_1tpz, 118515-80-3; C_2ppz, 118515-90-5; C_2pz, 118537-32-9; C_2tpz, 118515-91-6; D_1phz, 118516-09-9; D_1ppz, 118516-07-7; D_2phz, 118516-10-2; D_2ppz, 118516-08-8; E_1ppz, 118515-93-8; E_1pz, 78713-20-9; E_1tpz, 95662-22-9; E_2ppz, 118515-94-9; E_2pz, 78724-29-5; E_2tpz, 118515-95-0; $Pt_2Cl_4(C_2H_4)_2$, 12073-36-8; $Pt_2Cl_4(PEt_3)_2$, 15692-96-3; $Pt_2Cl_4(PMe_2Ph)_2$, 15699-79-3; $Pt_2Cl_4(PMePh_2)_2$, 16633-87-7; $Pt_2Cl_4(P\text{-}n\text{-}Bu_3)_2$, 15670-38-9.

Supplementary Material Available: For E_2ppz and A_2ppz, Table S1 (thermal factors), Table S2 (calculated hydrogen atom positions), Table S3 (extended list of bond distances and angles), and Table S5 (experimental data for the X-ray diffraction studies) (12 pages); Table S4 (listings of F_o and F_c) (20 pages). Ordering information is given on any current masthead page.

Contribution from the Istituto per lo Studio della Stereochimica ed Energetica dei Composti di Coordinazione, CNR, Firenze, Italy, Dipartimento di Chimica dell'Università di Pisa, Pisa, Italy, and Dipartimento di Scienze della Terra dell'Università di Perugia, Perugia, Italy

The Electron-Deficient Planar Tetrairon Cluster $Fe_4(CO)_8L_4$ (L = Pyridine)

Carlo Mealli,*[1] Davide Maria Proserpio,[1] Giuseppe Fachinetti,*[2] Tiziana Funaioli,[2] Giovanni Fochi,[2] and Pier Francesco Zanazzi[3]

Received June 10, 1988

A 56-electron cluster with formula $Fe_4(CO)_8(pyridine)_4$ (**1**) is formed by addition of $FeCl_2$ and $Na_2Fe(CO)_4$ in tetrahydrofuran containing a small excess of pyridine. The compound, which has a magnetic moment of 3.8 μ_B, has been structurally characterized. Crystal data for $C_{28}H_{20}N_4O_8Fe_4$: a = 21.511 (3) Å, b = 16.766 (3) Å, c = 19.253 (3) Å, β = 117.94 (2)°, monoclinic $P2_1/a$, Z = 8, R = 0.06 for 2848 observed reflections. The structure consists of a triangulated parallelogram of iron atoms, two of which are coordinated, at opposite vertices, each by four carbon monoxide molecules and the other two are each coordinated by two pyridine molecules. The Fe-Fe separations along the periphery are an average of 2.534 (4) Å, a length attributable to an Fe-Fe single bond. The length of the shortest diagonal is 2.759 (3) Å, raising the question whether there is residual Fe-Fe bonding along that direction. The question is examined by extended Hückel calculations. Simple qualitative MO arguments describe the interactions between opposite pairs of L_2Fe and L_4Fe fragments. Although they do not give a uniquely defined electronic ground-state configuration, significant pieces of information on the Fe-Fe trans-diagonal bond and on the electron distribution over the four metal atoms may be attained.

Introduction

As a part of our studies of the interaction of Lewis bases with metal carbonyl complexes,[4,5] we have observed that pyridine can induce the disproportionation of $Fe(CO)_5$ to yield the new cluster $Fe_4(CO)_8(py)_4$ (**1**). The preliminary characterization of the latter has been communicated.[5b] Now we report a straightforward method to synthesize **1** along with the results of a new single-crystal diffraction study. The number of valence electrons (56) indicates an electron deficiency which has been examined by semiempirical calculations. Within this context we present a new graphical computer program that allows threedimensional plottings of single molecular orbitals, as a whole or as a composite by separated atomic orbitals (or their hybrids). For these features the program written by C.M. and D.M.P. has been named CACAO (computer aided composition of atomic orbitals).[6]

Results

Synthesis. A few iron carbonyl complexes containing direct metal-metal bonds with elements from groups 11, 12, and 14 are known.[7] These complexes can be easily prepared by addition of

(1) CNR.
(2) Dipartimento di Chimica dell'Università di Pisa.
(3) Dipartimento di Scienza della Terra dell'Università di Perugia.
(4) Hieber, W. *Adv. Organomet. Chem.* **1970**, *8*, 1.
(5) (a) Fachinetti, G.; Fochi, G.; Funaioli, T. *J. Organomet. Chem.* **1986**, *301*, 91. (b) Fachinetti, G.; Fochi, G.; Funaioli, T.; Zanazzi, P. F. *J. Chem. Soc. Chem. Comm.* **1987**, 89. (c) Fachinetti, G.; Fochi, G.; Funaioli, T.; Zanazzi, P. F. *Angew. Chem., Int. Ed. Engl.* **1987**, *26*, 680. (d) Fachinetti, G.; Funaioli, T.; Marcucci, M. *J. Organomet. Chem.* Submitted for publication.
(6) Mealli, C.; Proserpio, D. M. To be submitted for publication.
(7) Shriver, D. F.; Whitmire, K. H. *Comprehensive Organometallic Chemistry*; Wilkinson, G., Ed.; Pergamon: Oxford, England, 1982; Vol. 4, pp 306-311.

0020-1669/89/1328-1122$01.50/0

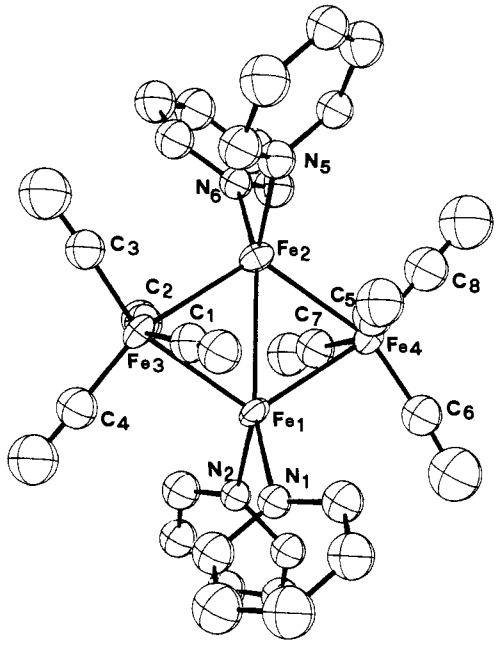

Figure 1. ORTEP drawing of one of the two independent cluster molecules in the crystal of $Fe_4(CO)_8(py)_4$

a metal halide to the iron tetracarbonyl dianion. Accordingly, we found that the reaction of $FeCl_2$ with $Na_2Fe(CO)_4$ in THF containing a small excess of pyridine, results in the formation of **1**, which is characterized by IR spectroscopy (ν_{CO} = 1968 s, 1909 s, 1890 s, 1606 w cm^{-1}), elemental analysis, and X-ray diffraction. In spite of the rather low yield (30%), this method, due to the ready availability of starting materials, allows the preparation of **1** in quantities much larger than those obtainable with the previously described procedure:[5b] namely the disproportionation of $Fe(CO)_5$ with pyridine. In the absence of pyridine, the new reaction leads to dark brown solutions that show IR absorptions very close, in the wavenumbers and relative intensities, (ν_{CO} = 1970 s, 1916 s, 1890 s cm^{-1}) to the characteristic pattern of **1**. However attempts to isolate the product analougous to **1**, $Fe_4(CO)_8(THF)_4$, invariably yield chloride-containing solids. Moreover such solutions are unstable at room temperature, and slow precipitation of the iron metal is observed therefrom. This suggests that THF does not have the necessary strength as a base (two-electron donor) to stabilize the unusual framework of **1**. The latter is paramagnetic with a magnetic moment corresponding to two unpaired spins (μ_{eff} = 3.8 μ_B). As additional pieces of information we report that **1** is EPR silent and that oxidation and reduction processes are irreversible on the cyclic voltammetry time scale.

Description of the Structure. There are two independent molecules of $Fe_4(CO)_8(py)_4$ in the asymmetric unit, and they present only marginal geometric differences.

Figure 1 shows one of these molecules in which the planar Fe_4 skeleton closely approximates a rhombus. Selected bond distances and angles are reported in Table I. The rhombus side averages 2.543 (4) Å, and the shortest Fe–Fe diagonal is 2.759 (3) Å. The latter vector connects the Fe_1 and Fe_2 atoms coordinated each by two pyridine molecules. It has to be established whether the latter iron atoms can be considered bonded or not. It is noteworthy that each FeN_2 plane is practically perpendicular to the Fe_4 skeleton. The other metal atoms, related by the longest diagonal (>4.2 Å) are coordinated each by four carbonyl ligands. The geometry of $Fe(CO)_4$ group is somewhat intermediate between tetrahedron and that of a typical butterfly ML_4 fragment, which descends from an octahedron after removal of two equatorial ligands. In fact one C–Fe–C angle (that formed by the CO ligands above and below the Fe_4 plane) is 148.2 (9)°, whereas the angle formed by the equatorial CO ligands averages 104.7 (9)°. The latter angular values recall a coordination geometry similar to that of the pseudooctahedral dihydridoiron tetracarbonyl.[9] Another interesting geometric detail is that the two equatorial CO ligands do not lie exactly in the Fe_4 plane since the two FeC_2 groupings are rotated, in opposite directions, by ≈6° with respect to that plane. It is to be established whether this feature is a result of steric or electronic effects. The result of our EHMO[8] study (vide infra), are not affected significantly by such a deformation. Other geometrical features that are worth noticing are (i) the Fe–N bonds, averaging 2.145 (12) Å, are intermediate between the Fe–N (pyridine) bonds found in some Fe(II) high spin complexes such as $FeCl_2(py)_4$[10] [2.296 (6) Å] and that found in the low-spin complex $Fe(CO)_4(py)$[11] where the Fe–N bond is as short as 2.046 (5) Å, (ii) and in view of probable steric hindrance between the pyridine rings, the average value [88.2 (10)°] of the N–Fe–N angles is surprisingly small.

Table I. Selected Bond Lengths (Å) and Angles (deg) for $Fe_4(CO)_8(py)_4$

		molecule a	molecule b
Fe(1)–Fe(2)	[(Fe(5)–Fe(6)]	2.757 (3)	2.761 (3)
Fe(1)–Fe(3)	[Fe(5)–Fe(7)]	2.543 (3)	2.538 (2)
Fe(1)–Fe(4)	[Fe(5)–Fe(8)]	2.545 (2)	2.548 (3)
Fe(2)–Fe(3)	[Fe(6)–Fe(7)]	2.539 (2)	2.540 (2)
Fe(2)–Fe(4)	[Fe(6)–Fe(8)]	2.544 (3)	2.550 (2)
Fe(1)–N(1)	[Fe(5)–N(5)]	2.152 (12)	2.153 (12)
Fe(1)–N(2)	[Fe(5)–N(6)]	2.145 (9)	2.136 (8)
Fe(2)–N(3)	[Fe(6)–N(7)]	2.138 (12)	2.154 (8)
Fe(2)–N(4)	[Fe(6)–N(8)]	2.139 (8)	2.144 (12)
Fe(3)–C(1)	[Fe(7)–C(29)]	1.705 (18)	1.758 (18)
Fe(3)–C(2)	[Fe(7)–C(30)]	1.748 (14)	1.437 (18)
Fe(3)–C(3)	[Fe(7)–C(31)]	1.715 (25)	1.727 (22)
Fe(3)–C(4)	[Fe(7)–C(32)]	1.696 (24)	1.711 (25)
Fe(4)–C(5)	[Fe(8)–C(33)]	1.774 (18)	1.730 (19)
Fe(4)–C(6)	[Fe(8)–C(34)]	1.694 (23)	1.756 (19)
Fe(4)–C(7)	[Fe(8)–C(35)]	1.732 (18)	1.727 (20)
Fe(4)–C(8)	[Fe(8)–C(36)]	1.735 (19)	1.731 (22)
Fe(3)–Fe(1)–Fe(4)	[Fe(7)–Fe(5)–Fe(8)]	114.3 (1)	114.3 (1)
Fe(3)–Fe(2)–Fe(4)	[Fe(7)–Fe(6)–Fe(8)]	114.4 (1)	114.2 (1)
Fe(1)–Fe(3)–Fe(2)	[Fe(5)–Fe(7)–Fe(6)]	65.7 (1)	65.9 (1)
Fe(1)–Fe(4)–Fe(2)	[Fe(5)–Fe(8)–Fe(6)]	65.6 (1)	65.6 (1)
N(1)–Fe(1)–N(2)	[N(5)–Fe(5)–N(6)]	89.2 (4)	88.7 (4)
N(3)–Fe(2)–N(4)	[N(7)–Fe(6)–N(8)]	86.7 (4)	88.2 (4)
C(1)–Fe(3)–C(2)	[C(29)–Fe(7)–C(30)]	148.5 (8)	147.2 (9)
C(3)–Fe(3)–C(4)	[C(31)–Fe(7)–C(32)]	104.9 (10)	103.6 (10)
C(5)–Fe(4)–C(7)	[C(33)–Fe(8)–C(34)]	149.4 (8)	147.9 (8)
C(6)–Fe(4)–C(8)	[C(35)–Fe(8)–C(36)]	104.5 (9)	105.9 (9)
Fe(2)–Fe(1)–N(1)	[Fe(6)–Fe(5)–N(5)]	135.5 (3)	135.0 (2)
Fe(2)–Fe(1)–N(2)	[Fe(6)–Fe(5)–N(6)]	135.2 (3)	136.3 (3)
Fe(1)–Fe(2)–N(3)	[Fe(5)–Fe(6)–N(7)]	136.5 (3)	137.5 (3)
Fe(1)–Fe(2)–N(4)	[Fe(5)–Fe(6)–N(8)]	136.8 (3)	134.3 (3)

Discussion

Description of the Bonding in $Fe_4(CO)_8(py)_4$. A few tetranuclear clusters having a quasi-planar M_4 skeleton and no capping or interstitial ligands are known. Their bonding description is not simple. The number of valence electrons is as low as 56 in $Mo_4Cl_8[P(OCH_3)_3]_4$ species,[12] where triple Mo≡Mo and single Mo—Mo bonds alternate, or is as large as 64 in $Pt_4(acetate)_8$[13] or $Os_4(CO)_{16}$.[14] The latter two compounds both have a slightly puckered square skeleton and are the closest inorganic equivalents of cyclobutane. In addition there are a number of 62 electron species where the metal–metal bonding interplay is variable. For example the $Re_4(CO)_{16}^{2-}$ species[15] has a diamond shape with five equivalent Re–Re bonds (one coinciding with the shortest diagonal of the rhombus) whereas the Os_4 species,[16a-b] with the same

(8) Hoffmann, R.; Lipscomb, W. N. *J. Chem. Phys.* **1962**, *36*, 2179, 3489; **1962**, *37*, 2872. Hoffmann, R. *Ibid.* **1963**, *39*, 1397.
(9) McNeill, E. A.; Scholor, F. R. *J. Am. Chem. Soc.* **1977**, *99*, 6243.
(10) Long, G. J.; Clarke, P. J. *Inorg. Chem.* **1978**, *17*, 1394.
(11) Cotton, F. A.; Troup, J. M. *J. Am. Chem. Soc.* **1974**, 96, 3438.
(12) Cotton, F. A.; Powell, G. L. *Inorg. Chem.* **1983**, *22*, 871.
(13) Carrondo, M. A. A. F. de C. T.; Skapski, A. C. *Acta Crystallogr., Sect. B* **1978**, *B34*, 1857, 3576.
(14) Johnston, V. J.; Einstein, F. W. B.; Pomeroy, R. K. *J. Am. Chem. Soc.* **1987**, *109*, 8111.
(15) Churchill, M. R.; Bau, R. *Inorg. Chem.* **1968**, *7*, 2606.

Table II. Crystallographic Data for $Fe_4(CO)_8(py)_4$

$C_{28}H_{20}N_4O_8Fe_4$	mol wt = 763.89
a = 21.511 (3) Å	$P2_1/a$ (No. 14)
b = 16.766(3) Å	T = 25 °C
c = 19.253(3) Å	λ = 0.71069 Å
β = 117.94 (2)°	ρ_{calcd} = 1.611 g cm^{-3}
V = 6134.3 Å^3	μ = 16.2 cm^{-1}
Z = 4	transmissn coeff = 0.98–0.88
$R(F_o)$ = 0.060	$R_w(F_o)$ = 0.069

electron count, presents at least three different types of metal–metal interactions. This holds for some Ru_4 planar clusters as well.[17] Some of us are investigating in full the above series of compounds from the theoretical point of view.[18]

In this paper we wish to limit our considerations to the compound $Fe_4(CO)_8(py)_4$ (**1**). The present iron cluster has a total of 56 valence electrons like $Mo_4Cl_8[P(OCH_3)_3]_4$[12] but also has a completely different bonding network and a paramagnetic nature. Our analysis, based on the extended Hückel method[8] and fragment orbital analysis,[19] addresses some major aspects of the cluster's nature. For example, since the compound was synthesized with the aim of finding new types of interaction between homonuclear ion pairs (HNIP)[5a-d], namely $Fe(CO)_4^{2-}$ and $(py)_nFe^{2+}$, one wonders whether the distinction between d^{10} and d^6 metals remains in the cluster. One wishes to identify the main metal–metal bonding interactions within the Fe_4 cycle and to check whether the shortest diagonal of the rhombus can be interpreted as a single, though weakened, Fe–Fe bond. Finally the origin of the paramagnetism and the site of the unpaired electrons can be discussed.

It has been shown for a class of trinuclear clusters that the metal–metal bonding and antibonding orbitals can be identified by seeking an analogy with the C–C interactions in cyclopropane.[20] In the present case the reference molecule, to compare $Fe_4(CO)_8(py)_4$ with, is cyclobutane (see I). As described in text-

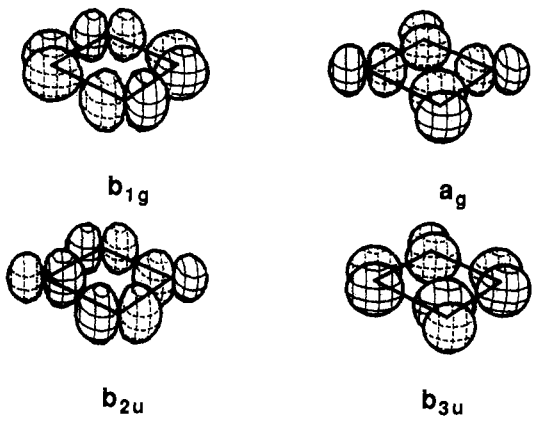

I

books[21] each carbon atom has radial r and tangential t orbitals that, in a delocalized MO picture, nest together to give four σ and four σ^* MO combinations. Only the former bonding set is shown in I. For later convenience, the labels are appropriate to the D_{2h} symmetry of the rhombus.

Our model for the Fe_4 cluster is shown in II and uses NH_2^- ligands in place of pyridines. As a further simplification, four CO ligands are rigidly kept in the equatorial Fe_4 plane. The strategy is that of analyzing the bonding interactions between the fragments $Fe_2(CO)_8$ and $Fe_2(NH_2)_4$. After the identification of

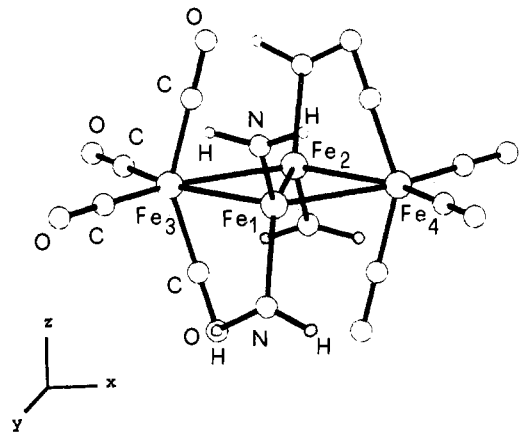

II

four cyclic Fe_4 bonding interactions with features as those in I, the residual bonding (if any) along the diagonal of the rhombus (Fe(1)–Fe(2)) can be identified.

As shown in III, fragment $Fe_2(CO)_8$ has four relevant in-phase (p) and out-of-phase (op) combinations of the σ (radial) and π (tangential) frontier orbitals typical of L_4M fragments with a

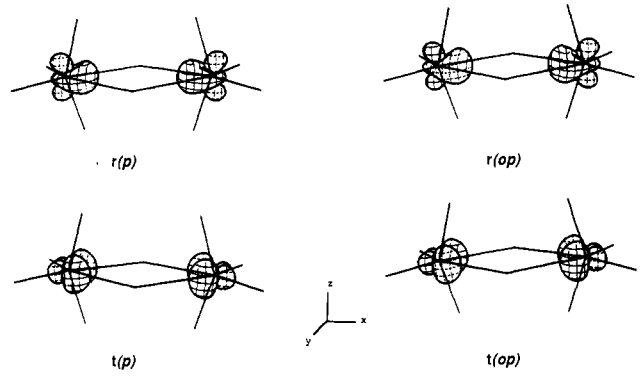

III

butterfly shape (C_{2v} symmetry). No major consequences are introduced by the bending of two trans axial ligands from a 180° angle to ≈148°.

While all of the combinations in III participate in the formation of the four cyclic Fe–Fe bonds, more difficult is to envisage the orbitals used by each $(NH_2)_2Fe$ fragment to reconstruct a scheme similar to I. Two of the nine metal basis orbitals (s, p, d) are used for σ M–N bonds (in first approximation these are s and p_z orbitals). There remain seven orbitals on each metal, shown in ascending order in IV. Those having antisymmetric character

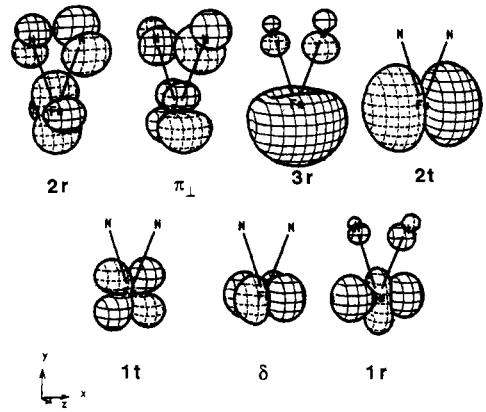

IV

with respect to the Fe_4 plane (xz is of δ, yz of $\pi_\perp$ type) do not contribute to the Fe_4 σ bond formation. Three of the remaining orbitals, with r character (various hybrids of $x^2 - y^2$, z^2, p_y, and

(16) (a) Johnston, V. J.; Einstein, F. W. B.; Pomeroy, R. K. *J. Am. Chem. Soc.* **1987**, *109*, 7220. (b) Martin, R. L.; Einstein, F. W. B.; Pomeroy, R. K. *Ibid.* **1986**, *108*, 338.
(17) Carty, A. J.; MacLaughlin, S. A.; Wagner, J.; Taylor, N. J. *Organometallics* **1982**, *1*, 1013.
(18) Mealli, C.; Proserpio, D. M. Manuscript in preparation.
(19) Fujimoto, H.; Hoffmann, R. *J. Chem. Phys.* **1964**, *78*, 1167.
(20) Mealli, C. *J. Am. Chem. Soc.* **1985**, *107*, 2245.
(21) Albright, T. A.; Burdett, J. K.; Whangbo, M. H. *Orbital Interactions in Chemistry*; Wiley: New York, 1975; p 189.

Table III. Fractional Atomic Coordinates in $Fe_4(CO)_8(py)_4$[a]

atom	x/a	y/b	z/c	atom	x/a	y/b	z/c
Fe(1)	0.0894 (1)	0.2545 (1)	0.1769 (1)	Fe(5)	−0.2878 (1)	0.2554 (1)	−0.3244 (1)
Fe(2)	−0.0383 (1)	0.2634 (1)	0.1776 (1)	Fe(6)	−0.4164 (1)	0.2690 (1)	−0.3260 (1)
Fe(3)	0.0644 (1)	0.3546 (1)	0.2599 (1)	Fe(7)	−0.3938 (1)	0.1713 (1)	−0.4125 (1)
Fe(4)	−0.0137 (1)	0.1634 (1)	0.0941 (1)	Fe(8)	−0.3107 (1)	0.3555 (1)	−0.2394 (1)
O(1)	0.1137 (1)	0.2109 (8)	0.3545 (7)	O(9)	−0.3259 (7)	0.0855 (8)	−0.2635 (8)
O(2)	−0.0147 (7)	0.4344 (7)	0.1102 (7)	O(10)	−0.4433 (7)	0.3187 (8)	−0.5022 (7)
O(3)	0.0010 (8)	0.4330 (8)	0.3479 (8)	O(11)	−0.5305 (10)	0.0929 (10)	−0.4856 (10)
O(4)	0.1999 (10)	0.4310 (10)	0.3142 (9)	O(12)	−0.3161 (8)	0.1046 (9)	−0.4903 (9)
O(5)	0.0279 (7)	0.0838 (7)	0.2455 (7)	O(13)	−0.2964 (6)	0.2151 (7)	−0.1444 (7)
O(6)	0.0646 (8)	0.0689 (8)	0.0354 (8)	O(14)	−0.3488 (6)	0.4349 (7)	−0.3901 (7)
O(7)	−0.0342 (6)	0.3031 (7)	−0.0045 (7)	O(15)	−0.1667 (8)	0.4139 (8)	−0.1556 (9)
O(8)	−0.1582 (9)	0.1032 (9)	0.0102 (9)	O(16)	−0.3894 (8)	0.4523 (9)	−0.1813 (8)
N(1)	0.1353 (5)	0.3098 (6)	0.1108 (5)	N(5)	0.2609 (5)	0.1886 (5)	0.6127 (5)
N(2)	0.1844 (5)	0.1873 (6)	0.2407 (5)	N(6)	0.3050 (4)	0.3150 (5)	0.7370 (5)
N(3)	−0.0879 (5)	0.2055 (5)	0.2376 (5)	N(7)	−0.5110 (4)	0.3386 (6)	−0.3868 (5)
N(4)	−0.1334 (4)	0.3305 (5)	0.1168 (5)	N(8)	−0.4633 (5)	0.2136 (6)	−0.2615 (5)
C(1)	0.0949 (10)	0.2704 (11)	0.3154 (10)	C(29)	−0.3512 (10)	0.1240 (11)	−0.3204 (11)
C(2)	0.0158 (8)	0.3976 (9)	0.1671 (9)	C(30)	−0.4238 (10)	0.2600 (11)	−0.4638 (11)
C(3)	0.0279 (10)	0.3990 (11)	0.3125 (11)	C(31)	−0.4737 (12)	0.1222 (12)	−0.4537 (12)
C(4)	0.1441 (12)	0.3988 (12)	0.2922 (12)	C(32)	−0.3513 (10)	0.1317 (11)	−0.4606 (11)
C(5)	0.0141 (9)	0.1193 (10)	0.1878 (10)	C(33)	−0.3046 (10)	0.2700 (11)	−0.1863 (10)
C(6)	0.0323 (10)	0.1092 (11)	0.0594 (10)	C(34)	−0.3348 (9)	0.3992 (10)	−0.3314 (10)
C(7)	−0.0237 (9)	0.2476 (10)	0.0377 (10)	C(35)	−0.2254 (11)	0.3908 (11)	−0.1911 (11)
C(8)	−0.0984 (10)	0.1251 (11)	0.0457 (10)	C(36)	−0.3584 (9)	0.4130 (10)	−0.2064 (10)
C(9)	0.1612 (5)	0.2589 (6)	0.0730 (5)	C(37)	0.2254 (5)	0.1830 (5)	0.5308 (5)
C(10)	0.1782 (5)	0.2891 (6)	0.0165 (5)	C(38)	0.2513 (5)	0.1336 (5)	0.4920 (5)
C(11)	0.1693 (5)	0.3701 (6)	−0.0022 (5)	C(39)	0.3128 (5)	0.0898 (5)	0.5351 (5)
C(12)	0.1434 (5)	0.4209 (6)	0.0356 (5)	C(40)	0.3483 (5)	0.0955 (5)	0.6169 (5)
C(13)	0.1264 (5)	0.3907 (6)	0.0921 (5)	C(41)	0.3224 (5)	0.1449 (5)	0.6557 (5)
C(14)	0.1829 (5)	0.1041 (6)	0.2430 (5)	C(42)	0.3355 (4)	0.3282 (5)	0.8178 (5)
C(15)	0.2438 (5)	0.0619 (6)	0.2918 (5)	C(43)	0.3918 (4)	0.3811 (5)	0.8538 (5)
C(16)	0.3062 (5)	0.1028 (6)	0.3383 (5)	C(44)	0.4176 (4)	0.4208 (5)	0.8089 (5)
C(17)	0.3077 (5)	0.1859 (6)	0.3360 (5)	C(45)	0.3871 (4)	0.4075 (5)	0.7280 (5)
C(18)	0.2468 (5)	0.2281 (6)	0.2872 (5)	C(46)	0.3308 (4)	0.3547 (5)	0.6921 (5)
C(19)	−0.0534 (5)	0.1922 (5)	0.3186 (5)	C(47)	−0.5104 (4)	0.4213 (6)	−0.3943 (5)
C(20)	−0.0826 (5)	0.1406 (5)	0.3523 (5)	C(48)	−0.5723 (4)	0.4616 (6)	−0.4437 (5)
C(21)	−0.1462 (5)	0.1023 (5)	0.3051 (5)	C(49)	−0.6347 (4)	0.4192 (6)	−0.4855 (5)
C(22)	−0.1807 (5)	0.1156 (5)	0.2242 (5)	C(50)	−0.6353 (4)	0.3364 (6)	−0.4780 (5)
C(23)	−0.1515 (5)	0.1672 (5)	0.1904 (5)	C(51)	−0.5734 (4)	0.2962 (6)	−0.4287 (5)
C(24)	−0.1712 (4)	0.3357 (5)	0.0350 (4)	C(52)	−0.4711 (5)	0.1310 (6)	−0.2614 (5)
C(25)	−0.2273 (4)	0.3889 (5)	0.0000 (5)	C(53)	−0.4907 (5)	0.0957 (6)	−0.2089 (5)
C(26)	−0.2457 (4)	0.4369 (5)	0.0466 (5)	C(54)	−0.5025 (5)	0.1429 (6)	−0.1566 (5)
C(27)	−0.2080 (4)	0.4318 (5)	0.1284 (5)	C(55)	−0.4947 (5)	0.2255 (6)	−0.1567 (5)
C(28)	−0.1518 (4)	0.3785 (5)	0.1634 (5)	C(56)	−0.4751 (5)	0.2609 (6)	−0.2091 (5)

[a] Estimated standard deviations in parentheses refer to the last digit.

s), are candidates to form a_g and b_{2u} combinations, whereas two others, with t character, (xy and p_x) are candidates to form the b_{1g} and b_{3u} MOs.

The diagram for the interaction between the fragments $Fe_2(CO)_8$ and $Fe_2(NH_2)_4$ is complicated, and it will be presented only in part at a later stage. At the moment we focus on six frontier MOs fairly isolated in the energy scale and packed with a 1-eV range (see V). A total of four electrons are available to them;

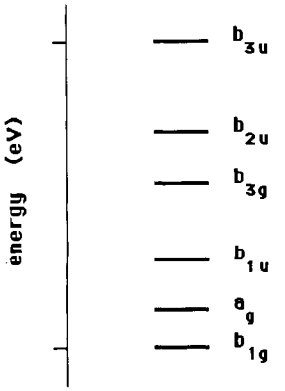

V

thus, the calculation itself is consistent with the paramagnetic nature of the cluster.

Table IV. Atomic Parameters Used in the Calculations

atom	orbital	H_{ii}, eV	ζ_1	ζ_2	C_1[a]	C_2[a]
Fe	4s	−9.10	1.90			
	4p	−5.32	1.90			
	3d	−12.60	5.35	2.00	0.5505	0.6260
N	2s	−26.0	1.95			
	2p	−13.4	1.95			
O	2s	−32.3	2.275			
	2p	−14.8	2.275			
C	2s	−21.4	1.625			
	2p	−11.4	1.625			
H	1s	−13.6	1.30			

[a] These are the coefficients in the double-ζ expansion.

In the absence of a detailed experimental study of the magnetism, it cannot be properly established whether the observed room-temperature magnetic moment of 3.8 μ_B corresponds to a triplet ground state with two unpaired electrons or is the result of a more complicate distribution of the electrons (for example a mixture of singlet and quintuplet states). However due to the inadequacy of the investigational method, we dismiss a detailed analysis of the possible electron configurations generating non-triplet states. Moreover even for triplet states the analysis is limited to check their consistency with some geometric features of the cluster. Such a goal requires a clear understanding of the makeup of the levels in V. Two of them, namely b_{1u} and b_{3g}, are essentially $\pi_\perp$ and $\pi_\perp^*$ combinations of $Fe_2(NH_2)_4$ yz hybrids and remain

extraneous to the Fe_4 σ-bonding network. These are shown in VI.

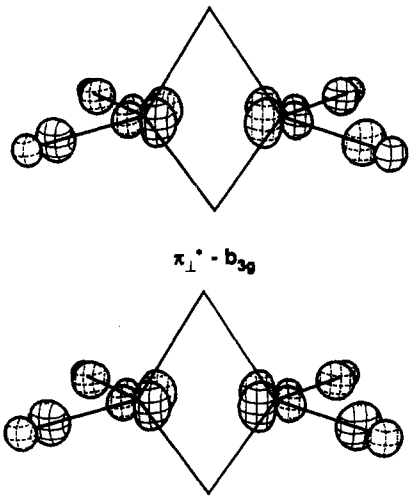

VI

Remarkably, the remaining b_{1g}, a_g, b_{2u}, and b_{3u} σ levels match the symmetries of the cyclobutane σ bonding orbitals, shown in I. A simplified viewpoint is to consider each of the four σ frontier MOs as an intermediate σ_2 level resulting from a typical three-orbital interaction, schematized in VII. On the left side fmo can

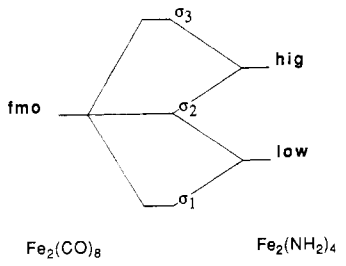

VII

be any of the four $Fe_2(CO)_8$ combinations in III, whereas the hig and low partners of $Fe_2(NH_2)_4$ are symmetry-adapted combinations of either the three r or the two t fragment orbitals in IV. Of the three resulting MOs, σ_2 may represent either a bonding (fmo/hig) or an antibonding (fmo/low) level. A two-orbital/two-electron interaction is established between fmo and low when there are no electrons in σ_2, with hig being totally excluded from the bonding interplay. In this case the two bonding electrons would be provided by the $Fe_2(NH_2)_4$ fragment.

Conversely, two electrons in σ_2 favour a fmo–hig bonding interaction of which σ_3 is the antibonding counterpart. In this case σ_1, mainly centered on low, can be taken as a lone pair on $Fe_2(NH_2)_4$ while the fragment $Fe_2(CO)_8$ acts as a donor toward $Fe_2(NH_2)_4$. It is important to stress that whatever is the population of the σ_2 type levels, the Fe_4 σ cyclic bonding network is assured.

As stated, we consider only triplet ground states, and in doing so, we exclude those configurations where the higher levels b_{3g}, b_{2u}, and b_{3u} can become populated. Most restrictively, we focus on the configurations $(b_{1g})^2(a_g)^1(b_{1u})^1$ and $(b_{1g})^1(a_g)^2(b_{1u})^1$. As shown in VI, the levels b_{1u} and b_{3g} have $\pi_\perp$ and $\pi_\perp^*$ characters, respectively; thus, one electron in the former triggers some $\pi_\perp$ bonding between the iron atoms coordinated by pyridines. Also notice that the latter MOs both exhibit a clear-cut Fe–N σ^* character that may affect somewhat the Fe–N distances. The 2.15 (1) Å average value in **1** is intermediate between that found in monomeric octahedral high spin complexes of iron [e.g. 2.229 (6) Å in $FeCl_2(py)_4$[10]] and that found in the diamagnetic complex $Fe(CO)_4(py)$,[11] which is as small as 2.046 (5) Å. The trend can be accounted for if we consider that (i) in the octahedral complexes the e_g levels having Fe–L σ^* character are singly occupied, (ii) no σ^* level is occupied in the diamagnetic complex, (iii) in **1** the σ^* Fe–N character is almost equally shared by the levels b_{1u} and b_{3g} distributed over the two $Fe(NH_2)_2$ centers. Since for the assumed configurations only one $\pi_\perp$ level (b_{1u}) is singly populated, the Fe–N σ antibonding power is halved with respect to that of the reference high-spin monomer. A second electron in any of the $\pi_\perp$ levels lowers significantly the calculated Fe–N overlap population.

Next we wish to understand which major geometric differences are introduced by adopting the two alternative triplet configurations containing either $(a_g)^2$ or $(b_{1g})^2$. The overlap population analysis shows that the diagonal Fe–Fe bond is most sensitive to the electrons in a_g. In fact the corresponding calculated overlap raises from 0.13 to 0.15 in switching from the $(b_{1g})^2(a_g)^1(b_{1u})^1$ to the $(b_{1g})^1(a_g)^2(b_{1u})^1$ configuration. These values compare with 0.17, the calculated overlap population for the peripheral Fe–Fe bonds.

A three-dimensional drawing of the MO a_g, VIII, shows clearly trans-diagonal bonding overlap between the two iron atoms coordinated by nitrogen donors. Recall however that, according

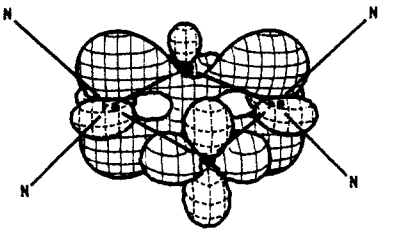

a_g

VIII

to the simplified scheme VII, the filled a_g level could also be regarded as the overall radial orbital bonding between the fragmental orbitals fmo and hig (i.e. σ_2). In other words a_g could have the same function as the cyclobutane analogue, which provides one-fourth of the cyclic bonding network.

In order to make this point less intriguing we present the simplified interaction diagram IX, which reports on the right side

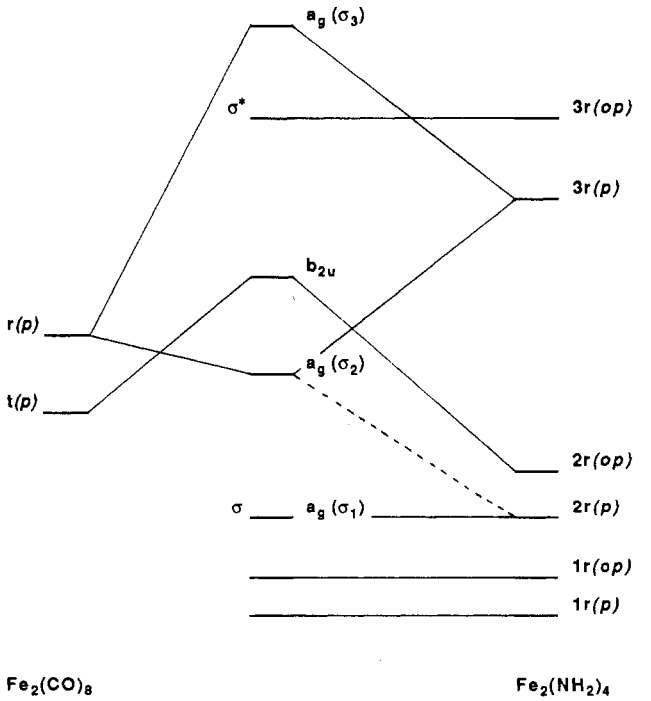

IX

only the in-phase (p) and out-of-phase (op) combinations of the radial hybrids of each $Fe(NH_2)_2$ group. These may also be taken as three σ/σ^* pairs for the potential Fe–Fe diagonal bonding. On the left side of IX, we show two FMOs from $Fe_2(CO)_8$ (already seen in III), which may interact with the FMOs of $Fe_2(NH_2)_4$

to provide two-fourths of the overall Fe_4 cyclic bond. The important point to be made is that, for energy match and overlap reasons, only 2r(op) and 3r(p) interact largely with the $Fe_2(CO)_8$ FMOs; hence, they take part in the formation of the Fe_4 cyclic bond. The pairs 1r(p)/1r(op) and 2r(p)/3r(op) remain largely unaffected. The former pair, being fully populated, is uneffective, but the latter is at the origin of a two-orbital/two-electron interaction that triggers substantial σ bonding between the transdiagonal metal atoms. However, second-order perturbation effects mix the composition of the MOs $a_g(\sigma_1)$ and $a_g(\sigma_2)$, which lose much of their original character. In particular, the two MOs share both the Fe_4 and diagonal Fe–Fe σ-bonding character. The situation is not dissimilar from that typical of bridged metal dimers [e.g. $Fe_2(CO)_9$] where the distinction between direct metal–metal and metal–ligand (bridge) bonding orbitals becomes quite unclear.[22]

A final comment can be devoted to the relative assignment of electrons to the two types of metal in the cluster. If the HNIP hypothesis is valid, the four frontier electrons should all belong to the iron–carbonyl fragments (fmo's in VII), thus allowing a distinction between d^{10} and d^6 electron counts. In view of the previous arguments the situation may be quite different. Any electron in the $\pi_\perp$ level (b_{1u}) must be assigned to the pyridine iron atoms. Also, upon rehybridization with the lower $a_g(\sigma_1)$ level, $a_g(\sigma_2)$ acquires the Fe(1)–Fe(2) bonding character, clearly seen in VIII. In spite of being so close in energy to the $Fe_2(CO)_8$ fmo, the MO $a_g(\sigma_2)$ receives only a 42% contribution from the latter group. The Mulliken population analysis confirms an almost even distribution of charges among the four metal atoms for both the triplet states under consideration. This suggests that all of the four metal atoms are not far from a d^8 configuration. In conclusion, the cluster's formation changes greatly the distribution of the electrons with respect to that of the combining original species [$Fe(CO)_4$ anions and Fe(II) pyridine cationic complexes]. Upon multiple Fe–Fe covalent bonding formation and coupling of the Fe(II) unpaired spins, the presence of HNIPs is no longer realistic. The observed precipitation of iron metal on decomposition of the THF specimen seems to confirm indirectly such a conclusion.

Experimental Section

General Data. All manipulations were carried out under prepurified argon by using standard Schlenk techniques. Infrared spectra were recorded on a Perkin-Elmer Model 283 instrument using an 0.1-mm CaF_2 cell. Tetrahydrofuran and diethyl ether were purified by distillation from $LiAlH_4$. Pyridine was distilled from CaH_2 after 24 h of reflux. Commercial $FeCl_2 \cdot 4H_2O$ was dried in vacuo (220 °C; 5×10^{-2} mmHg). The product of the continuous THF extraction of the dried salt had a THF content of 46.0% ($FeCl_2 \cdot 1.5THF$). $Na_2Fe(CO)_4$ was prepared as described in the literature[22] and was purified by continuous THF extraction. Quantitative determination of pyridine was performed by gas chromatographic comparison (Fractovap 2450 apparatus with HWD detector) with standards; samples were treated with KOH in CH_3OH before analysis. Quantitative analyses of iron were performed in aqueous Fe^{2+} solution by complexometric method (EDTA; PAN). The aqueous Fe^{2+} solutions were obtained on treatment of samples with I_2/CH_3OH followed by addition of 1:1 aqueous HNO_3. Yellow, clean solutions were obtained on boiling. Quantitative analyses of CO were performed measuring gas evolved on treatment of samples with I_2/py. Magnetic susceptibilities of solid samples were measured on a Faraday balance.

Preparation of $Fe(CO)_8(py)_4$. To 150 cm^3 of THF pyridine (1.9 cm^3, 23.57 mmol) were added $FeCl_2 \cdot 1.5THF$ (1.83 g, 7.79 mmol) and $Na_2Fe(CO)_4$ (1.66 g, 7.76 mmol) in this order. The mixture was stirred vigorously for 3 h, then it was filtered to give a clear brown solution to which 300 cm^3 of diethyl ether were superimposed, and only slow mixing due to diffusion was allowed. After the mixture was allowed to stand overnight, dark brown crystals were formed, collected on a filter, and dried in vacuo (yield 0.89 g, 30%). Anal. Calcd for $Fe_4(CO)_8(py)_4$: py, 41.4; Fe, 29.26; CO, 29.34. Found: py, 42.1; Fe, 29.07; CO, 28.90.

X-ray Data Collection and Structure Determination. A crystal with dimension 0.20 × 0.13 × 0.05 mm protected in a glass capillary was mounted on a computer-controlled Philips PW1100 single-crystal diffractometer, equipped with graphite-monochromatized Mo Kα radiation. A summary of crystal data is presented in Table II. The intensities were collected at room temperature up to $2\theta = 40°$; the ω–2θ scan technique was employed, the scan range being 1.2° and the speed 0.04° s^{-1}. A total of 6204 reflections were measured, but owing to the poor quality and the small dimensions of the crystal only 2848 with $I > 2\sigma(I)$ could be considered *observed* and retained for subsequent calculations. Two standard reflections, which were measured periodically, showed no apparent variation in Lorentz and polarization factors. A semiempirical absorption correction was applied on the basis of the variation in intensity during the azimuthal scans of some reflections according to the method of North et al.;[24] the transmission factors were in the range 0.98–0.88.

The structure was solved by Patterson and direct methods and refined by a full-matrix least-squares methods with the SHELX-76 package of programs.[25] Owing to the unfavorable observations-to-parameters ratio the pyridine molecules were constrained to perfect hexagons (edge length = 1.395 Å). The contributions of H atoms at the calculated positions were included, with an overall isotropic thermal parameter that refined to 0.16 $Å^2$. Anisotropic thermal parameters were refined only for the Fe atoms. The refinement converged to an R value of 0.060 for 2848 observations and 299 parameters. The R(weighted) was 0.069 ($R_w = (\sum_w(|F_o| - |F_c|)^2)^{1/2}/(\sum wF_o^2)^{1/2}$, $w = (\sigma^2(F_o))^{1/2}$). A ΔF map at the late stage of refinement is essentially featureless. Atomic coordinates are given in Table III.

Computational Details. All of the MO calculations were of the extended Hückel type using a modified version of the Wolfsberg–Helmholz formula. The atomic parameters used are summarized in Table IV. The model used has the following geometric features: Fe–Fe(cyclic) = 2.539 Å; Fe–Fe(diagonal) = 2.756 Å; Fe–C = 1.71 Å; Fe–N = 2.14 Å; C–O = 1.15 Å; N–H = 1.0 Å; angles of rhombus, 114.3 and 65.7°; C–Fe–C(equatorial) = 105°; C–Fe–C(axial) = 148°; N–Fe–N = 90°. The three-dimensional graphic plots of the orbitals have been performed by a computer program named CACAO (computer aided composition of atomic orbitals) written in the Fortran language by D.M.P. and C.M. A detailed description will be reported elsewhere.[6]

Acknowledgment. We are grateful to Drs. Piero Zanello and Franco Laschi of the Universitâ di Siena for attempting EPR and electrochemical characterization of the compound.

Registry No. 1, 107766-76-7; $Na_2Fe(CO)_4$, 14878-31-0; $Fe_4(CO)_8(NH_2)_4$, 119144-90-0.

Supplementary Material Available: Table S1 (complete crystal data), Tables S2 and S3 (thermal parameters), and Table S4 (calculated coordinates of hydrogen atoms) (4 pages); a table of observed and calculated structure factors (16 pages). Ordering information is given on any current masthead page.

(22) Summerville, R. H.; Hoffmann, R. *J. Am. Chem. Soc.* **1979**, *101*, 3821.
(23) Collman, J. P.; Finke, R. G., Cawse, J. N.; Brauman, J. N. *J. Am. Chem. Soc.* **1977**, *99*, 2515.
(24) North, A. C. T.; Phillips, D. C.; Mathews, F. S. *Acta Crystallogr., Sect. A* **1968**, *A24*, 351.
(25) Sheldrick, G. M. "SHELX76, Program for Crystal Structure Determinations"; University of Cambridge: Cambridge, England, 1976.